

BAD: BIDIRECTIONAL AUTO-REGRESSIVE DIFFUSION FOR TEXT-TO-MOTION GENERATION

Seyed Rohollah Hosseini¹, Ali Ahmad Rahmani², Seyed Jamal Seyedmohammadi³, Sanaz Seyedin¹, Arash Mohammadi³

¹Dept. of Electrical Engineering, Amirkabir University of Technology (AUT), Tehran, Iran

²Dept. of Electrical Engineering, Iran University of Science and Technology (IUST), Tehran, Iran

³Concordia Institute of Information Systems Engineering (CIISE), Concordia University, Montreal, Canada

ABSTRACT

Autoregressive models excel in modeling sequential dependencies by enforcing causal constraints, yet they struggle to capture complex bidirectional patterns due to their unidirectional nature. In contrast, mask-based models leverage bidirectional context, enabling richer dependency modeling. However, they often assume token independence during prediction, which undermines the modeling of sequential dependencies. Additionally, the corruption of sequences through masking or absorption can introduce unnatural distortions, complicating the learning process. To address these issues, we propose Bidirectional Autoregressive Diffusion (BAD), a novel approach that unifies the strengths of autoregressive and mask-based generative models. BAD utilizes a permutation-based corruption technique that preserves the natural sequence structure while enforcing causal dependencies through randomized ordering, enabling the effective capture of both sequential and bidirectional relationships. Comprehensive experiments show that BAD outperforms autoregressive and mask-based models in text-to-motion generation, suggesting a novel pre-training strategy for sequence modeling. The codebase for BAD is available on <https://github.com/RohollahHS/BAD>.

Index Terms— Motion Generation - Autoregressive Models - Mask-based Generative Models - Diffusion Models

1. INTRODUCTION

Text-to-motion generation [1–5] is an emerging field that integrates natural language processing with 3D human motion synthesis, offering substantial potential for applications in gaming, film industry, virtual reality, and robotics [6–8]. This task is inherently challenging due to the difficulty of mapping discrete textual descriptions into continuous, high-dimensional motion data. To address this challenge, Vector-Quantized Variational Autoencoders (VQ-VAEs) [9] have proven to be particularly effective in text-to-motion generation [10–12]. Typically, a two-stage approach is followed where a VQ-VAE is first trained to transform continuous motion data into discrete motion tokens. In the second stage and to model the distribution of motion tokens in discrete space, either autoregressive or denoising models are employed. Nevertheless, despite their effectiveness, each category has its inherent limitations as outlined below.

Literature Review: Autoregressive models excel at capturing and leveraging sequential dependencies on various modalities [13–18] due to their reliance on the causality of the input. In these models, each token is predicted based on previously generated tokens, allowing the model to naturally learn the progression and relationship between consecutive tokens. Employing autoregressive models to learn discrete motion sequences has led to significant improvements in text-to-motion generation, generating high-fidelity and coherent motion sequences [11, 19, 20]. The unidirectional nature of these

models, however, limit their ability to fully capture deep bidirectional context, as they only consider the preceding tokens lacking insight into the future ones.

Conversely, denoising models, particularly mask-based generative models [21] or absorbing diffusion models [22], leverage both preceding and subsequent contexts to capture rich bidirectional relationships, eliminating unidirectional bias. By adopting this approach, mask-based motion models [12, 23] enhance the generation of complex motion sequences over autoregressive motion models. Mask-based generative models, however, assume that masked tokens are conditionally independent [24], meaning predictions do not account for potential dependencies between masked tokens, which can result in suboptimal predictions. Furthermore, the corruption process in these models involves transitioning certain tokens in the input sequence to a [MASK] token or an absorbed state. Encoding a portion or the entire sequence into a fully masked (absorbed) form is an unnatural process, which distorts the sequence and complicates the task of learning the corresponding reverse noise-to-data mapping.

Contributions: Motivated by the aforementioned limitations of autoregressive and mask-based generative models, we propose the Bidirectional Autoregressive Diffusion (BAD) framework, a novel pretraining strategy for sequence modeling that unifies the strengths of both autoregressive and mask-based generative models. We evaluate BAD in the context of text-to-motion generation in a two-stage process. In the first stage, we train a motion tokenizer based on the conventional VQ-VAE to convert motion sequences into discrete representations using a learned codebook. In the second stage, the proposed BAD is used to train a transformer architecture. This process begins with a novel corruption method designed based on permutation operation. Specifically, we utilize multiple different mask tokens (absorbed states) and a random ordering to systematically corrupt the sequence, resulting in a more natural corrupted sequence. After randomly masking a portion of the motion sequence, a hybrid attention mask, which integrates a permuted causal attention mask and a bidirectional attention mask, is constructed to determine the dependencies among input tokens. The permuted causal attention mask enforces each masked token to learn its causal dependencies on others, while the bidirectional attention mask ensures that all tokens can attend to both preceding and subsequent unmasked tokens, therefore, enriching the model’s capacity to capture sequential dependencies and deep bidirectional context.

Although our primary goal is to address issues related to autoregressive and mask-based generative models using the proposed BAD framework, we demonstrate that by using a simple VQ-VAE as our motion tokenizer in the first stage, our model can achieve competitive or superior results compared to models employing advanced VQ-VAEs, such as Residual Vector Quantization (RVQ) [25], used

in [23, 26]. In RVQ-VAE, multiple layers of vector quantization are applied sequentially, with each layer encoding residual information not captured by the preceding layers. Such a hierarchical approach significantly enhances the performance of the motion tokenizer and, consequently, that of the overall framework. Using RVQ-VAE, however, often requires training multiple transformers and incurs additional network calls during inference to predict motion tokens associated with the residual layers in the second stage. These will greatly increase the computational complexity and training time of the underlying model. In contrast, the proposed framework, which uses a simple VQ-VAE as its motion tokenizer, requires training only a single transformer in the second stage. Furthermore, it requires far fewer number of network calls during inference, while achieving comparable results to RVQ-VAE-based models. In summary, the paper makes the following key contributions:

- Introduction of BAD framework, which integrates the bidirectional capabilities of mask-based generative models with the causal dependencies inherent in autoregressive modeling.
- Introduction of a novel corruption (diffusion) technique for discrete data in the context of text-to-motion generation. The proposed technique, unlike prior works, preserves the sequential nature of data, facilitating a more natural learning process.

Extensive experiments are performed based on widely recognized text-to-motion HumanML3D [4] and KIT-ML [27] datasets. Our results demonstrate the superiority of the proposed BAD framework against autoregressive and mask-based motion baseline models. Specifically, we improve the Fréchet Inception Distance (FID) of [12], a mask-based generative motion model, from 0.089 to 0.049 on HumanML3D and from 0.316 to 0.221 on KIT-ML dataset, while maintaining a similar model size and design choices. We also show that BAD achieves comparable results to methods utilizing advanced motion tokenizers, highlighting its efficiency and effectiveness. Finally, we show that BAD performs quite well on other tasks, such as text-guided motion inpainting and outpainting.

2. THE BAD FRAMEWORK

Our objective is to develop a text-to-motion generation framework that, given a textual description, generates coherent and complex human motion sequences. As illustrated in Fig. 1, the proposed framework consists of two main components: (i) A motion tokenizer (Section 2.1), and; (ii) A conditional transformer (Section 2.2). The motion tokenizer converts raw 3D motion into discrete tokens, while the transformer predicts the original tokens from a corrupted sequence, conditioned on a text prompt. During inference (Section 2.3), given a text prompt, the transformer starts with a noise vector \mathbf{z} and iteratively denoises it to generate a motion sequence.

2.1. Motion Tokenizer

The motion tokenizer, illustrated in Fig. 1(a), comprises of an encoder and a decoder. Consider a raw motion sequence $F = \{f_1, f_2, \dots, f_\tau\}$ with τ frames, where $f_t \in \mathbb{R}^D$ denotes the motion vector with dimensionality of D at frame t . The encoder maps the raw motion sequence F into a continuous latent space, yielding $E = \{e_1, e_2, \dots, e_T\}$ with $T = \tau/l$, where $e_t \in \mathbb{R}^d$ is the latent vector with dimensionality of d , and l is the temporal downsampling rate. To obtain a discrete representation, each latent vector e_t is mapped to the nearest vector in a learned codebook $\mathcal{C} = \{c_k \in \mathbb{R}^d \mid k = 1, 2, \dots, K\}$, where K is the number of codebook entries. The quantized latent vector is defined as $x_t = \text{Quantize}(e_t) = c_k$, where $k = \arg \min_j \|e_t - c_j\|$. Finally, the decoder receives the quantized or discrete motion sequence

$X = \{x_1, x_2, \dots, x_T\}$ to reconstruct the raw motion sequence $\hat{F} = \{\hat{f}_1, \hat{f}_2, \dots, \hat{f}_\tau\}$. The objective function for training the VQ-VAE is given by

$$L_{vq} = \|F - \hat{F}\|_1 + \|\text{sg}[E] - X\|_2 + \beta \|E - \text{sg}[X]\|_2, \quad (1)$$

where β controls the commitment loss, and $\text{sg}(\cdot)$ denotes the stop-gradient operation.

2.2. Conditional Mask-Based Transformer

Our transformer is designed to model the distribution of discrete motion tokens conditioned on a given textual description. The associated textual description is first processed through a pre-trained Contrastive Language-Image Pretraining (CLIP) model [28], yielding sentence and word embeddings that capture both global and local relationships between the text and motion sequence. Sentence embedding is prepended to the motion sequence, and word embeddings are integrated via cross-attention at the begging of the transformer.

Corruption Process: Let \mathcal{Z}_T denote the set of all possible permutations of the sequence $[1, 2, \dots, T]$, where T is the sequence length. We define the p -th element of a permutation $\mathbf{z} \in \mathcal{Z}_T$ as z_p , with the first p elements as $\mathbf{z}_{\leq p}$ and the last $T-p+1$ elements as $\mathbf{z}_{\geq p}$.

Given a discrete motion sequence $X = (x_1, x_2, \dots, x_T)$, we first randomly select n_m candidate motion tokens to be masked, resulting in a corrupted motion sequence composed of masked tokens X_m and unmasked tokens X_u . Using X_u , a bidirectional attention mask att_{bi} is created, which allows all tokens to attend to unmasked tokens from both directions. Next, we sample a random ordering $\mathbf{z} \sim \mathcal{Z}_T$ to determine the order of all T mask tokens $\mathbf{m} = (m_1, m_2, \dots, m_T)$, where $m_i \in \mathbb{R}^d$, from our Maskbook. Using \mathbf{z} , the corresponding permuted causal attention mask att_{per} is created, which enforces that each mask token m_{z_p} at position z_p can only attend to the last $T-p+1$ mask tokens, denoted by $\mathbf{m}_{\mathbf{z}_{\geq p}}$. Finally, the candidate masked tokens X_m are replaced with n_m randomly selected mask tokens, and the hybrid attention mask is constructed as $\text{att}_{\text{hyb}} = \text{att}_{\text{bi}} + \text{att}_{\text{per}}$. The hybrid attention mask ensures that mask tokens attend only to $\mathbf{m}_{\mathbf{z}_{\geq p}}$, maintaining causal dependencies similar to autoregressive models. Additionally, mask tokens can attend to unmasked tokens, while unmasked tokens only attend to each other. By attending to both the left and right unmasked tokens, our transformer effectively captures bidirectional context, similar to BERT [21]. Fig. 2 illustrates examples of the hybrid attention masks.

Note: Following previous works, we use random replacement augmentation by replacing $c_r \times 100\%$ of ground-truth motion tokens with random ones before masking, where $c_r \sim U(0, 0.4)$. The number of tokens for masking, n_m , is also obtained as $c_m \times 100\%$ of the sequence length, where c_m is sampled from $U(0, 0.5)$ with a probability of 0.1 or $U(0.5, 1)$ with a probability of 0.9. n_m can also be prepended to the motion sequence, denoted as *time* in Fig. 1(b).

Objective Function: Our objective function is expressed as follows

$$\max_{\theta} \mathbb{E}_{\mathbf{z} \sim \mathcal{Z}_T} \sum_{z_p=1}^T \left\{ \begin{array}{l} m' \log p_{\theta}(x_{z_p} \mid \mathbf{m}_{\mathbf{z}_{\geq p}}, X_u) \\ (1 - m') \log p_{\theta}(x_{z_p} \mid X_u) \end{array} \right. \quad (2)$$

where $m' = 1$ if x_{z_p} is masked. The first part of Eq. (2) aligns with the autoregressive objective, thus avoiding the independence assumption of masked tokens during prediction. For the sake of simplicity, other conditions, including S (sentence embedding), W (word embeddings), and t (time), have been omitted from Eq. (2).

2.3. Inference

Given the permutation-based nature of our procedure, the proposed model can be trained under either $\mathbf{m}_{\mathbf{z}_{\geq p}}$ or $\mathbf{m}_{\mathbf{z}_{\leq p}}$ condition. Under

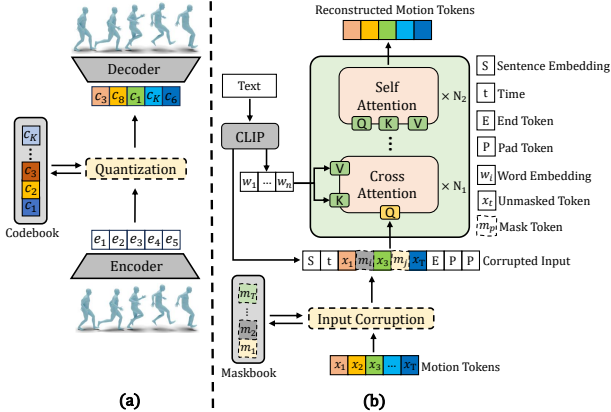


Fig. 1: Overall framework of our text-to-motion model. (a) Motion tokenizer, transforms a raw 3D motion sequence into a sequence of discrete motion tokens. (b) The conditional mask-based transformer reconstructs original discrete motion tokens from a corrupted sequence conditioned on a text prompt.

$\mathbf{m}_{z \leq p}$ condition, the mask tokens should attend to the first p mask tokens. Different generation methods can then be applied using the same trained model. In this paper, we demonstrate two of such methods. Each generation method can employ parallel decoding, where the transformer decodes all mask tokens while selectively masking others based on a cosine scheduling function, $n_m = T \cos(\frac{1}{2} \pi i / I)$, where i and I represent the current iteration and the total number of iterations, respectively. Initially, a high masking ratio is applied, masking most of the motion tokens. As the generation process progresses, the masking ratio is gradually reduced, increasing the available context. This increasing context allows the model to infer the remaining masked tokens more accurately. To determine the number of mask tokens n_m at each iteration i , we need the sequence length T . This sequence length can also be masked and learned by the model, which requires minor modifications. However, since our goal is to propose BAD, we aim to keep everything simple. Alternatively, one can use a length estimator or pre-specify T .

2.3.1. Order-Agnostic Autoregressive Sampling (OAAS)

In this approach, we first sample a random ordering $\mathbf{z} \sim \mathcal{Z}_T$ to create mask tokens and the corresponding permuted causal attention mask. Decoding begins from m_{z_1} , allowing this token to attend to all other mask tokens $\mathbf{m}_{z \geq 1}$ and use the rich information they captured during training. In the subsequent iterations, the hybrid attention mask is updated, and mask tokens are allowed to attend only to the last $T-p+1$ mask tokens $\mathbf{m}_{z \geq p}$ and unmasked tokens. This iterative process continues until all tokens are decoded. Alternatively, for the model under $\mathbf{m}_{z \leq p}$ condition, decoding starts from m_{z_T} .

2.3.2. Confidence-Based Sampling (CBS)

This approach also initiates generation from randomly ordered mask tokens based on a random ordering $\mathbf{z} \sim \mathcal{Z}_T$. During decoding, tokens predicted with high confidence are retained, while lower-confidence tokens are masked for further processing. This ensures that the sequence benefits from the most reliable predictions, potentially enhancing the quality of the generated sequence.

3. EXPERIMENTS

Datasets: We conducted experiments using two widely recognized text-to-motion datasets: (i) HumanML3D dataset [4], a large-scale dataset with 14,616 motion sequences and 44,970 textual descriptions, combining data from AMASS [29], and HumanAct12 [30], and; (ii) KIT-ML dataset [27], a smaller benchmark with 3,911 motion sequences and 6,278 textual annotations, sourced from the KIT [31] and CMU [32] motion databases.

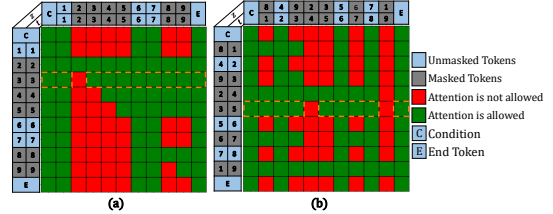


Fig. 2: Examples of two different hybrid attention masks. \mathbf{z} represents a random ordering $\mathbf{z} \sim \mathcal{Z}_T$, while t denotes time. Each mask token attends to the last $T-p+1$ mask tokens $\mathbf{m}_{z \geq p}$ and unmasked tokens. For example, orange cells indicate tokens that the third mask token, m_{z_3} , can attend to, including unmasked tokens and the existing $\mathbf{m}_{z \geq 3}$ mask tokens.

Evaluation Metrics: For evaluations, we use standard metrics from previous works [4], leveraging pre-trained models to encode text and motion features. We assess the alignment between generated motions and text prompts using R-Precision, reporting Top-1, Top-2, and Top-3 accuracies. To evaluate motion quality, we calculate Fréchet Inception Distance (FID) to measure the distributional difference between generated and real motion features. We also assess diversity by computing the average Euclidean distance between randomly selected pairs of generated motions and Multimodality by measuring variance across multiple motions generated from the same prompt. These metrics together provide a comprehensive understanding of the quality and diversity of the generated motions relative to the text prompt.

Implementation Details: Following [12], we use a simple VQ-VAE motion tokenizer with a codebook size of 8,192 and a dimension of 32, along with a temporal downsampling rate of $l = 4$. For training, motion sequences from HumanML3D and KIT-ML datasets are truncated to a length of $\tau = 64$. The model is optimized using AdamW optimizer with $[\beta_1, \beta_2] = [0.9, 0.99]$, a batch size of 256, and an exponential moving average constant $\lambda = 0.99$. We initially train for 200K iterations using a learning rate of 2×10^{-4} , then continue for another 100K iterations with a reduced learning rate of 1×10^{-5} . In the second stage, we use a transformer [33] consisting of 18 layers, each with a dimension of 1,024 and 16 attention heads. The first two layers are cross-attention layers, while the rest are self-attention layers. The transformer is also trained using AdamW with $[\beta_1, \beta_2] = [0.5, 0.99]$ and a batch size of 128. The learning rate is initially set at 2×10^{-4} for the first 150K iterations and is subsequently decayed to 1×10^{-5} for the rest of the training.

3.1. Comparison with state-of-the-art approaches

Quantitative Comparison: Following [4], we report the metrics as the average over 20 generation experiments, with a 95% confidence interval. We use $I = 10$ iterations during the generation process. To demonstrate the core effectiveness of the proposed approach, we deliberately avoid employing advanced VQ-VAE designs such as RVQ in the motion tokenizer. Table 1 shows that BAD, with a similar model size and design choices, consistently outperforms the baselines, T2M-GPT [11], an autoregressive motion model, and MMM [12], a mask-based generative motion model. By achieving the lowest FID score compared to T2M-GPT and MMM on both datasets, BAD demonstrates its ability to capture the sequential flow of information while simultaneously modeling rich bidirectional dependencies in complex motion sequences, indicating that the generated motions are natural and realistic. For text-motion consistency, BAD further improves R-Precision and MM-Dist metrics. In terms of inference speed, similar to MMM, BAD offers high inference speed compared to autoregressive [11, 19, 20] and diffusion-based motion models [3, 5, 34].

Table 2 compares BAD with two leading methods, Momask and

Dataset	Methods	R-Precision \uparrow			FID \downarrow	MM-Dist \downarrow	Diversity \uparrow	MModality \uparrow
		Top-1	Top-2	Top-3				
HumanML3D	Real	0.511 \pm .003	0.703 \pm .003	0.797 \pm .002	0.002 \pm .000	2.974 \pm .008	9.503 \pm .065	-
	VQ-VAE	0.505 \pm .002	0.697 \pm .003	0.790 \pm .002	0.085 \pm .001	3.031 \pm .009	9.650 \pm .073	-
	MDM [34]	0.320 \pm .005	0.498 \pm .004	0.611 \pm .007	0.544 \pm .044	5.566 \pm .027	9.559 \pm .086	2.799 \pm .072
	MotionGPT [20]	0.435 \pm .003	0.607 \pm .002	0.700 \pm .002	0.160 \pm .008	3.700 \pm .009	9.411 \pm .081	3.437\pm.091
	T2M-GPT [11]	0.491 \pm .003	0.680 \pm .003	0.775 \pm .002	0.116 \pm .004	3.118 \pm .011	9.761\pm.081	1.856 \pm .011
	AttT2M [19]	0.499 \pm .003	0.690 \pm .002	0.786 \pm .002	0.112 \pm .006	3.038 \pm .007	9.700\pm.090	2.452 \pm .051
	MMM [12]	0.515 \pm .002	0.708 \pm .002	0.804 \pm .002	0.089 \pm .005	2.926 \pm .007	9.577 \pm .050	1.226 \pm .035
	BAD (CBS 2.3.2)	0.511 \pm .002	0.704 \pm .002	0.800 \pm .002	0.049\pm.003	2.957 \pm .006	9.688 \pm .089	1.119 \pm .042
BAD (OAAS 2.3.1)	0.517\pm.002	0.713\pm.003	0.808\pm.003	<u>0.065\pm.003</u>	2.901\pm.008	9.694 \pm .068	1.194 \pm .044	
KIT-ML	Real	0.424 \pm .005	0.649 \pm .006	0.779 \pm .006	0.031 \pm .004	2.788 \pm .012	11.080 \pm .097	-
	VQ-VAE	0.400 \pm .006	0.619 \pm .006	0.746 \pm .007	0.437 \pm .010	2.981 \pm .017	11.093 \pm .095	-
	MDM [34]	0.164 \pm .004	0.291 \pm .004	0.396 \pm .004	0.497 \pm .021	9.191 \pm .022	10.85 \pm .109	1.907 \pm .214
	MotionGPT [20]	0.366 \pm .005	0.558 \pm .004	0.558 \pm .005	0.510 \pm .016	3.527 \pm .021	10.35 \pm .084	2.328\pm.117
	T2M-GPT [11]	0.402 \pm .006	0.619 \pm .005	0.737 \pm .006	0.717 \pm .041	3.053 \pm .026	10.86 \pm .094	1.912 \pm .036
	AttT2M [19]	<u>0.413\pm.006</u>	0.632\pm.006	0.751\pm.006	0.870 \pm .039	3.039 \pm .021	<u>10.96\pm.123</u>	2.281\pm.047
	MMM [12]	0.404 \pm .005	0.621 \pm .005	0.744 \pm .004	0.316 \pm .028	2.977 \pm .019	10.91 \pm .101	1.232 \pm .039
	BAD (CBS 2.3.2)	0.408 \pm .004	0.612 \pm .007	0.734 \pm .007	<u>0.246\pm.019</u>	3.100 \pm .021	10.874 \pm .083	1.485 \pm .059
BAD (OAAS 2.3.1)	0.417\pm.006	<u>0.631\pm.006</u>	<u>0.750\pm.006</u>	0.221\pm.012	2.941\pm.025	11.000\pm.100	1.170 \pm .047	

Table 1: Quantitative evaluation on HumanML3D and KIT-ML test sets. Best results are in **bold**, with second-best underlined. The evaluation is repeated 20 times for each metric, and the mean is reported along with the 95% confidence interval, denoted by \pm .

Dataset	Methods	R-Precision \uparrow			FID \downarrow	MM-Dist \downarrow	Diversity \uparrow	MModality \uparrow
		Top-1	Top-2	Top-3				
HumanML3D	MoMask [23]	0.521	0.713	0.807	0.045	2.958	-	1.241
	BAMM [26]	0.525	0.720	0.814	0.055	2.919	9.717	1.687
	BAD (CBS)	0.511	0.704	0.800	0.049	2.957	9.688	1.119
	BAD (OAAS)	0.517	0.713	0.808	0.065	2.901	9.694	1.194
KIT-ML	MoMask [23]	0.433	0.656	0.781	0.204	2.779	-	1.131
	BAMM [26]	0.438	0.661	0.788	0.183	2.723	11.008	1.609
	BAD (CBS)	0.408	0.612	0.734	0.246	3.100	10.874	1.485
	BAD (OAAS)	0.417	0.631	0.750	0.221	2.941	11.000	1.170

Table 2: Quantitative evaluation on HumanML3D and KIT-ML test sets in comparison to RVQ-VAE-based models.

Task	Method	R-Precision			FID \downarrow	MM-Dist \downarrow	Diversity \uparrow
		Top-1	Top-2	Top-3			
Temporal Inpainting (In-betweening)	Momask	0.820	0.820	0.040	2.878	9.640	
	BAMM	0.821	0.056	2.863	9.629		
	BAD	0.810	0.045	2.899	9.546		
Temporal Outpainting	Momask	0.818	0.057	2.889	9.619		
	BAMM	0.822	0.056	2.856	9.659		
	BAD	0.800	0.034	2.961	9.579		
Prefix	Momask	0.822	0.06	2.875	9.607		
	BAMM	0.821	0.058	2.868	9.612		
	BAD	0.806	0.036	2.917	9.615		
Suffix	Momask	0.819	0.052	2.881	9.659		
	BAMM	0.814	0.050	2.891	9.721		
	BAD	0.808	0.044	2.909	9.593		

Table 3: Quantitative evaluation on temporal editing tasks on HumanML3D.

BAMM, both of which use RVQ in their motion tokenizers, greatly improving the motion tokenizer metrics and consequently the overall framework. On HumanML3D, which is a larger and, therefore, more reliable dataset than KIT-ML, we achieve a better FID score compared to BAMM while remaining quite close to Momask. For text-motion consistency, our approach achieves comparable performance (R-Precision and MM-Dist) to both BAMM and Momask. Given that our pre-training approach can be easily adapted to other models, we anticipate that using an RVQ-based motion tokenizer could further improve our results, which we leave to future work.

We tested four temporal editing tasks on HumanML3D dataset: motion inpainting (generating the central 50% of a sequence conditioned on the first and last 25%), outpainting (generating the middle portion from the start and end of the sequence), prefix prediction (generating the second half of the sequence from the initial 50%), and suffix completion (generating the beginning of the sequence from the final 50%). These tasks are crucial for assessing motion sequence coherence and are illustrated in Fig. 3(c), and Table 3. Results show that BAD outperforms advanced models Momask and BAMM in terms of FID score.

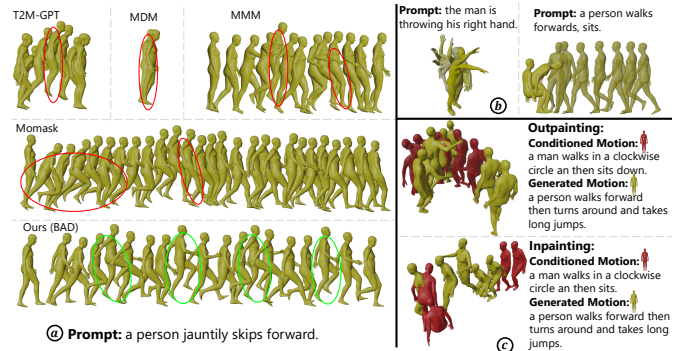


Fig. 3: Quality Comparison. (a) Visualization of generated motions from various models for the same prompt, with red circles indicating defects and green circles highlighting correct, natural motions. (b) Additional motions generated by BAD. (c) Visualization of temporal editing tasks.

Qualitative Comparison: Fig. 3(a) shows motions generated by different models for the same prompt. T2M-GPT and MDM fail to generate coherent motion, while MMM produces unnatural hand and foot movements, as indicated by the red circles. Momask initially generates a running motion, which is inconsistent with the prompt, and like MMM, fails to achieve natural hand and foot alignment. In contrast, BAD generates the motion with natural hand and foot movements and correctly performs the action multiple times.

4. CONCLUSION

We introduce BAD, a novel generative framework for text-to-motion generation, implemented in a two-stage process. First, a simple VQ-VAE is used to transform a raw 3D motion sequence into a sequence of discrete tokens. Next, a permutation-based corruption process corrupts the sequence, and a multi-layer transformer is trained to reconstruct it. By using a hybrid attention mask, our transformer captures rich bidirectional relationships while also learning causal dependencies between masked tokens. Extensive experiments demonstrate that BAD not only surpasses baseline approaches but also achieves competitive or superior results compared to RVQ-VAE-based models on various text-to-motion generation tasks. Notably, BAD can be easily adapted to other models and modalities, such as text, audio, and images.

5. REFERENCES

- [1] Zhiyuan Ren, Zhihong Pan, Xin Zhou, and Le Kang, “Diffusion motion: Generate text-guided 3d human motion by diffusion model,” in *ICASSP 2023 - 2023 IEEE International Conference on Acoustics, Speech and Signal Processing (ICASSP)*, 2023, pp. 1–5.
- [2] Mathis Petrovich, Michael J Black, and Gül Varol, “Temos: Generating diverse human motions from textual descriptions,” in *European Conference on Computer Vision*. Springer, 2022, pp. 480–497.
- [3] Xin Chen, Biao Jiang, Wen Liu, Zilong Huang, Bin Fu, Tao Chen, and Gang Yu, “Executing your commands via motion diffusion in latent space,” in *Proceedings of the IEEE/CVF Conference on Computer Vision and Pattern Recognition*, 2023, pp. 18000–18010.
- [4] Chuan Guo, Shihao Zou, Xinxin Zuo, Sen Wang, Wei Ji, Xingyu Li, and Li Cheng, “Generating diverse and natural 3d human motions from text,” in *Proceedings of the IEEE/CVF Conference on Computer Vision and Pattern Recognition*, 2022, pp. 5152–5161.
- [5] Mingyuan Zhang, Zhongang Cai, Liang Pan, Fangzhou Hong, Xinying Guo, Lei Yang, and Ziwei Liu, “Motiondiffuse: Text-driven human motion generation with diffusion model,” *arXiv preprint arXiv:2208.15001*, 2022.
- [6] Samaneh Azadi, Akbar Shah, Thomas Hayes, Devi Parikh, and Sonal Gupta, “Make-an-animation: Large-scale text-conditional 3d human motion generation,” in *Proceedings of the IEEE/CVF International Conference on Computer Vision*, 2023, pp. 15039–15048.
- [7] Chaoqun Gong, Yuqin Dai, Ronghui Li, Achun Bao, Jun Li, Jian Yang, Yachao Zhang, and Xiu Li, “Text2avatar: Text to 3d human avatar generation with codebook-driven body controllable attribute,” in *ICASSP 2024 - 2024 IEEE International Conference on Acoustics, Speech and Signal Processing (ICASSP)*, 2024, pp. 16–20.
- [8] Guy Tevet, Brian Gordon, Amir Hertz, Amit H Bermano, and Daniel Cohen-Or, “Motionclip: Exposing human motion generation to clip space,” in *European Conference on Computer Vision*. Springer, 2022, pp. 358–374.
- [9] Aaron van den Oord, Oriol Vinyals, and koray kavukcuoglu, “Neural discrete representation learning,” in *Advances in Neural Information Processing Systems*, I. Guyon, U. Von Luxburg, S. Bengio, H. Wallach, R. Fergus, S. Vishwanathan, and R. Garnett, Eds. 2017, vol. 30, Curran Associates, Inc.
- [10] Chuan Guo, Xinxin Zuo, Sen Wang, and Li Cheng, “Tm2t: Stochastic and tokenized modeling for the reciprocal generation of 3d human motions and texts,” in *European Conference on Computer Vision*. Springer, 2022, pp. 580–597.
- [11] Jianrong Zhang, Yangsong Zhang, Xiaodong Cun, Yong Zhang, Hongwei Zhao, Hongtao Lu, Xi Shen, and Ying Shan, “Generating human motion from textual descriptions with discrete representations,” in *Proceedings of the IEEE/CVF conference on computer vision and pattern recognition*, 2023, pp. 14730–14740.
- [12] Ekkasit Pinyoanuntapong, Pu Wang, Minwoo Lee, and Chen Chen, “Mmm: Generative masked motion model,” in *Proceedings of the IEEE/CVF Conference on Computer Vision and Pattern Recognition*, 2024, pp. 1546–1555.
- [13] Aaron Van Den Oord, Nal Kalchbrenner, and Koray Kavukcuoglu, “Pixel recurrent neural networks,” in *International conference on machine learning*. PMLR, 2016, pp. 1747–1756.
- [14] Keyu Tian, Yi Jiang, Zehuan Yuan, Bingyue Peng, and Liwei Wang, “Visual autoregressive modeling: Scalable image generation via next-scale prediction,” *arXiv preprint arXiv:2404.02905*, 2024.
- [15] Emiel Hoogeboom, Alexey A. Gritsenko, Jasmijn Bastings, Ben Poole, Rianne van den Berg, and Tim Salimans, “Autoregressive diffusion models,” in *International Conference on Learning Representations*, 2022.
- [16] Aaron Van Den Oord, Sander Dieleman, Heiga Zen, Karen Simonyan, Oriol Vinyals, Alex Graves, Nal Kalchbrenner, Andrew Senior, Koray Kavukcuoglu, et al., “Wavenet: A generative model for raw audio,” *arXiv preprint arXiv:1609.03499*, vol. 12, 2016.
- [17] Nal Kalchbrenner, Erich Elsen, Karen Simonyan, Seb Noury, Norman Casagrande, Edward Lockhart, Florian Stimberg, Aaron Oord, Sander Dieleman, and Koray Kavukcuoglu, “Efficient neural audio synthesis,” in *International Conference on Machine Learning*. PMLR, 2018, pp. 2410–2419.
- [18] Tom B Brown, “Language models are few-shot learners,” *arXiv preprint ArXiv:2005.14165*, 2020.
- [19] Chongyang Zhong, Lei Hu, Zihao Zhang, and Shihong Xia, “Att2m: Text-driven human motion generation with multi-perspective attention mechanism,” in *Proceedings of the IEEE/CVF International Conference on Computer Vision*, 2023, pp. 509–519.
- [20] Biao Jiang, Xin Chen, Wen Liu, Jingyi Yu, Gang Yu, and Tao Chen, “Motiongpt: Human motion as a foreign language,” *Advances in Neural Information Processing Systems*, vol. 36, 2024.
- [21] Jacob Devlin, Ming-Wei Chang, Kenton Lee, and Kristina Toutanova, “Bert: Pre-training of deep bidirectional transformers for language understanding,” 2019.
- [22] Jacob Austin, Daniel D Johnson, Jonathan Ho, Daniel Tarlow, and Rianne Van Den Berg, “Structured denoising diffusion models in discrete state-spaces,” *Advances in Neural Information Processing Systems*, vol. 34, pp. 17981–17993, 2021.
- [23] Chuan Guo, Yuxuan Mu, Muhammad Gohar Javed, Sen Wang, and Li Cheng, “Momask: Generative masked modeling of 3d human motions,” in *Proceedings of the IEEE/CVF Conference on Computer Vision and Pattern Recognition*, 2024, pp. 1900–1910.
- [24] Zhilin Yang, Zihang Dai, Yiming Yang, Jaime Carbonell, Russ R Salakhutdinov, and Quoc V Le, “Xlnet: Generalized autoregressive pretraining for language understanding,” in *Advances in Neural Information Processing Systems*, H. Wallach, H. Larochelle, A. Beygelzimer, F. d’Alché-Buc, E. Fox, and R. Garnett, Eds. 2019, vol. 32, Curran Associates, Inc.
- [25] Neil Zeghidour, Alejandro Luebs, Ahmed Omran, Jan Skoglund, and Marco Tagliasacchi, “Soundstream: An end-to-end neural audio codec,” *IEEE/ACM Transactions on Audio, Speech, and Language Processing*, vol. 30, pp. 495–507, 2021.
- [26] Ekkasit Pinyoanuntapong, Muhammad Usama Saleem, Pu Wang, Minwoo Lee, Srijan Das, and Chen Chen, “Bamm: Bidirectional autoregressive motion model,” *arXiv preprint arXiv:2403.19435*, 2024.
- [27] Matthias Plappert, Christian Mandery, and Tamim Asfour, “The kit motion-language dataset,” *Big data*, vol. 4, no. 4, pp. 236–252, 2016.
- [28] Alec Radford, Jong Wook Kim, Chris Hallacy, Aditya Ramesh, Gabriel Goh, Sandhini Agarwal, Girish Sastry, Amanda Askell, Pamela Mishkin, Jack Clark, et al., “Learning transferable visual models from natural language supervision,” in *International conference on machine learning*. PMLR, 2021, pp. 8748–8763.
- [29] Naureen Mahmood, Nima Ghorbani, Nikolaus F Troje, Gerard Pons-Moll, and Michael J Black, “Amass: Archive of motion capture as surface shapes,” in *Proceedings of the IEEE/CVF international conference on computer vision*, 2019, pp. 5442–5451.
- [30] Chuan Guo, Xinxin Zuo, Sen Wang, Shihao Zou, Qingyao Sun, Annan Deng, Minglun Gong, and Li Cheng, “Action2motion: Conditioned generation of 3d human motions,” in *Proceedings of the 28th ACM International Conference on Multimedia*, 2020, pp. 2021–2029.
- [31] Christian Mandery, Ömer Terlemeç, Martin Do, Nikolaus Vahrenkamp, and Tamim Asfour, “The kit whole-body human motion database,” in *2015 International Conference on Advanced Robotics (ICAR)*. IEEE, 2015, pp. 329–336.
- [32] CMU Graphics Lab, “Cmu graphics lab motion capture database,” <http://mocap.cs.cmu.edu/>, Accessed: 2022-11-11.
- [33] A Vaswani, “Attention is all you need,” *Advances in Neural Information Processing Systems*, 2017.
- [34] Guy Tevet, Sigal Raab, Brian Gordon, Yonatan Shafir, Daniel Cohen-Or, and Amit H. Bermano, “Human motion diffusion model,” 2022.